

Article

# Optimal Dispatch of High-Penetration Renewable Energy Integrated Power System Based on Flexible Resources

Jiawei Feng <sup>1</sup>, Junyou Yang <sup>1,\*</sup>, Haixin Wang <sup>1</sup>, Huichao Ji <sup>1</sup>, Martin Onyeka Okoye <sup>1</sup>, Jia Cui <sup>1</sup>, Weichun Ge <sup>2</sup>, Bo Hu <sup>2</sup> and Gang Wang <sup>3</sup>

<sup>1</sup> School of Electrical Engineering, Shenyang University of Technology, Shenyang 110870, China; jiawefeng\_sut@163.com (J.F.); haixinwang@sut.edu.cn (H.W.); huichaoji@neepu.edu.cn (H.J.); martinokoye@yahoo.com (M.O.O.); cuijiayouxiang@sut.edu.cn (J.C.)

<sup>2</sup> State Grid Liaoning Electric Power Supply Co. Ltd., Shenyang 110004, China; gwc@ln.sgcc.com.cn (W.G.); hubo\_dl@ln.sgss.com.cn (B.H.)

<sup>3</sup> Power Science Research Institute of State Grid Liaoning Electric Power Co. Ltd., Shenyang 110006, China; 18624063515@163.com

\* Correspondence: junyouyang@sut.edu.cn; Tel.: +86-139-4008-8191

Received: 23 May 2020; Accepted: 1 July 2020; Published: 3 July 2020



**Abstract:** The volatility and uncertainty of high-penetration renewable energy (RE) challenge the stability of the power system. To tackle this challenge, an optimal dispatch of high-penetration RE based on flexible resources (FRs) is proposed to enhance the ability of the power system to cope with uncertain disturbances. Firstly, the flexibility of a high-penetration RE integrated power system is analyzed. The flexibility margin of power supply and flexible adaptability of RE are then introduced as the evaluation indices for optimal operation. Finally, a multi-objective optimal dispatch model for power system flexibility enhancement based on FRs under the constraint of flexibility indices is proposed. The simulation results show that the proposed optimal dispatch can effectively enhance the flexibility of the power system and the penetration of RE and reduce pollutant emissions. Compared with the conventional method, the daily average emissions of CO<sub>2</sub>, SO<sub>2</sub>, and NO<sub>x</sub> with the proposed method are reduced by about 83,600 kg, 870 kg, and 370 kg, respectively, the maximum allowable volatility of net load is increased by 7.63%, and the average volatility of net load is reduced by 2.67%.

**Keywords:** flexibility evaluation indices; flexible resources; high-penetration renewable energy; interruptible load; optimal dispatch

## 1. Introduction

Due to the volatility and intermittence of renewable energy (RE), large-scale integration of RE into a power system increases the volatility of the system's net load, which causes the thermal power unit (TPU) to operate in a state of deep peak shaving and affects the economics and pollution of the power system [1,2]. Traditional resource flexibility can no longer meet the flexibility needs of high-penetration power systems [3]. Therefore, it is necessary to develop an optimal dispatch of a high-penetration RE integrated power system to enhance the system's flexibility [4].

At present, the complementary characteristics of RE and conventional energy sources such as gas power and thermal power are used to ensure the safe operation of power system [5,6]. In the high-penetration RE integrated system, it is difficult to effectively respond to the rapid change of the net load by relying solely on the reserve capacity, resulting in greater risks to the security of the power grid [7,8]. In [9,10], scholars point out that the effective management of FRs can improve flexibility and reduce the operation cost of the system. A multi-carrier energy dispatch optimization method based

on energy storage (ES) is proposed in [11]. The coordinated control of gas units and ES can increase system flexibility and reduce operation cost. ES and TPU models are considered in the presented models [12,13]. The energy response and ES in the real-time electricity market are considered in [14,15]. However, it is not enough to rely on ES and conventional power sources to provide flexibility. More flexible resources (FRs), such as interrupted loads, are required to participate in improving power system flexibility.

Configuring enough spare capacity can easily cause a lot of spare redundancy, which is expensive and unsustainable. In recent years, some scholars have analyzed the high-penetration RE integrated system from the perspective of flexibility [16,17]. Most of the researches on flexibility are based on principle analysis, qualitative evaluation, and lack of quantitative evaluation indices and modeling methods for power system flexibility. Reference [18] evaluates the flexibility by scoring different types of FRs, but the uncertainty of the FRs is not considered. It is only applicable to the rough assessment at the early stage of planning. Reference [19] proposes a new capacity expansion model, which considers ES and policy constraints, but the balance of a high-penetration RE power system is neglected. An improved real-time dispatch model is proposed to enhance system flexibility by operational flexibility metrics that lack slope probability [20]. The flexibility of power generation capacity is considered to improve the flexibility of the power system [21,22]. Furthermore, [23] proposes a method to improve system flexibility by reducing load levels. However, it ignores the issue that unit shutdown may be caused by excessive net load fluctuations. Although the flexibility of the traditional power system has been improved, there are still insufficient evaluation indices for the power system with high-penetration RE. The advantages and disadvantages of research on power system flexibility are shown in Table 1.

**Table 1.** Advantages and disadvantages of research on power system flexibility.

References	Models	Advantages	Disadvantages
FRs	Distributed dispatch model [5]	Multi-energy coordination and optimization	Ignore FRs in optimal dispatch
	Integrated ES model [9,10]	Considering FRs to participate in optimal dispatch	Ignore the connection between FRs and traditional resources
	Comprehensive centralized scheduling model [12–15]	Considering the coordination and optimization of ES and traditional resources	Ignore the diversity of FRs
	ES and load coordination model [18]	Considering multiple FRs to participate in optimal dispatch	Ignore the uncertainty of FRs
Flexibility Evaluation Indices	Capacity expansion model [19]	Combining system flexibility and policy constraints	Ignore system fluctuations caused by high-penetration RE
	Distributed energy resources aggregator optimization model [23]	FRs and load coordination and optimization	Ignore problems caused by large fluctuations in net load

FRs (Flexible Resources), ES (Energy storage), RE (Renewable energy).

This paper proposes comprehensive flexibility evaluation indices to enhance the flexibility of a high-penetration RE integrated power system. Flexibility evaluation indices quantify power system flexibility from time scale and directionality. A multi-objective optimal dispatch model of a high-penetration RE integrated power system with interruptible loads and ES is established. With the consideration of the proposed flexibility evaluation indices, the volatility of net load and pollution emissions are reduced through the accurate regulation of FRs.

The remaining part of this paper is organized as follows. Section 2 analyses the evaluation indices related to the flexibility of the power system. The dispatch model of a high-penetration RE integrated power system based on FRs is proposed in Section 3. In Section 4, the pollution and net load fluctuation results of different dispatch models in the simulation are compared. Finally, the conclusions are given in Section 5.

## 2. Flexibility Evaluation Indices of the Power System with High-Penetration RE

### 2.1. Power System Flexibility

At present, there is no standard definition of power system flexibility. The power system flexibility is mainly characterized by inherent attributes, directionality, and time correlation [24]. Power system flexibility is influenced by power supply side, grid side, load side, and ES. In this paper, the flexibility of the power system with RE is defined, as, within certain time scales, the power system quickly dispatches resources and responds to changes in the net load under the strictly economic and operational constraints. Net load indicates the sum of the total load, RE, and other FRs. The more flexible the power system, the more RE generation can be absorbed [25]. Increasing flexibility is beneficial to reducing pollution emissions and enhancing the economy of the power system.

Energy consumption is expected to increase at an additional annual rate of 10% [26]. The integration of high-penetration RE has become an inevitable trend [27,28]. The high-penetration RE will lead to frequent fluctuation of the net load and reduce the power system flexibility. Therefore, to enhance the power system flexibility, it is necessary to optimize the flexibility resources. The control actions are commonly used to optimize the flexibility of a power system at different time scales [24]. The control actions at different time scales are shown in Figure 1. Based on different time scales, the system has different levels of flexibility, which requires relevant control actions. A shorter time scale focuses on short-term flexibility operations and evaluation, and a longer time scale focuses on the system's ability to respond to changes over several years. This paper studies and analyzes the power system flexibility on an hourly time scale.

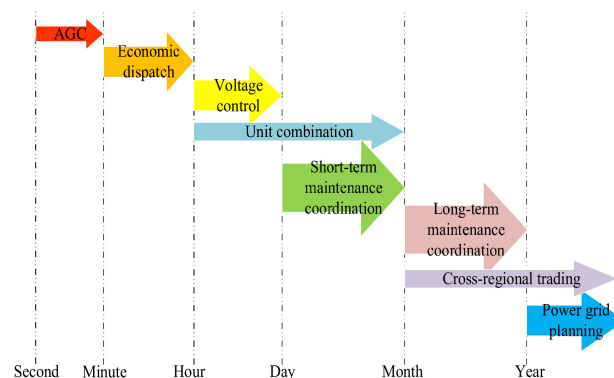


**Figure 1.** Control actions at different time scales.

### 2.2. Power System Flexibility Evaluation Indexes

This paper develops the comprehensive flexibility evaluation indices from the aspects of the power supply flexibility margin and flexible adaptability of grid-connected RE. Power supply flexibility margin considers the balance between supply and demand. Flexible adaptability of grid-connected RE considers the influence of RE on different time scales.

#### (1) Power Supply Flexibility Margin

Power supply side mainly relies on conventional power sources (e.g., TPUs, gas units, hydroelectric units) to achieve flexibility adjustment. The adjustable capacities of TPUs represent flexibility. In the process of load rise or fall, upward and downward adjustment flexibilities are expressed in Equations (1)–(6).

$$P_t^{su} = \sum_{m_t=1}^{M_t} P_{m_t,t}^u + \sum_{m_g=1}^{M_g} P_{m_g,t}^u \quad (1)$$

$$P_{m_t,t}^u = \min(P_{m_t}^+ - P_{m_t,t}, R_{m_t}^u) \quad (2)$$

$$P_{m_g,t}^u = \min(P_{m_g}^+ - P_{m_g,t}, R_{m_g}^u) \quad (3)$$

$$P_t^{\text{sd}} = \sum_{m_t=1}^{M_t} P_{m_t,t}^{\text{d}} + \sum_{m_g=1}^{M_g} P_{m_g,t}^{\text{d}} \quad (4)$$

$$P_{m_t,t}^{\text{d}} = \min(P_{m_t,t} - P_{m_t}^-, R_{m_t}^{\text{d}}) \quad (5)$$

$$P_{m_g,t}^{\text{d}} = \begin{cases} \min(P_{m_g,t} - P_{m_g}^-, R_{m_g}^{\text{d}}), & P_{m_g,t} \geq P_{m_g}^- \\ 0, & P_{m_g,t} \leq P_{m_g}^- \end{cases} \quad (6)$$

where  $P_t^{\text{su}}$  and  $P_t^{\text{sd}}$  are the upward and downward adjustment flexibilities of the power system at time  $t$ ,  $M_t$  is the total number of TPUs,  $P_{m_t,t}^u$  and  $P_{m_t,t}^{\text{d}}$  are the upward and downward adjustment flexibilities of TPU  $m_t$ ,  $P_{m_t,t}$  is the output of TPU  $m_t$ ,  $P_{m_t}^+$  and  $P_{m_t}^-$  are the upper and lower limits of the output,  $R_{m_t}^u$  and  $R_{m_t}^{\text{d}}$  are the climbing and descending capabilities,  $M_g$  is the total number of gas units,  $P_{m_g,t}^u$  and  $P_{m_g,t}^{\text{d}}$  are the upward and downward adjustment flexibilities of gas unit  $m_g$ ,  $P_{m_g,t}$  is the output of gas unit  $m_g$ ,  $P_{m_g}^+$  and  $P_{m_g}^-$  are the upper and lower limits of the output, and  $R_{m_g}^u$  and  $R_{m_g}^{\text{d}}$  are the climbing and descending capabilities, respectively. The power unit is MW and the climbing capability unit is MW/h.

The flexibility requirements of the power system in the process of load rise or fall are expressed in Equations (7) and (8).

$$P_t^{\text{du}} = w_u P_{t+1}^{\text{w}} + n_u P_L^{t+1} + (P_L^{t+1} - P_L^t) \quad (7)$$

$$P_t^{\text{dd}} = w_d (P_{\text{max}}^{\text{w}} - P_{t+1}^{\text{w}}) + n_d P_L^{t+1} + (P_L^t - P_L^{t+1}) \quad (8)$$

where  $P_t^{\text{du}}$  and  $P_t^{\text{dd}}$  are the requirements for the power system upward and downward adjustment flexibilities,  $w_u$  and  $w_d$  are the requirements of the wind power prediction error for upward and downward adjustment flexibilities,  $P_t^{\text{w}}$  is the prediction power of wind turbines,  $P_{\text{max}}^{\text{w}}$  is the maximum wind power prediction,  $n_u$  and  $n_d$  are the requirements of the load forecasting error for the upward and downward adjustment flexibilities, and  $P_L^t$  is the load.

According to the abovementioned supply and requirement flexibilities of the power system, the power supply flexibility margins are derived as in Equations (9) and (10).

$$P_t^{\text{mu}} = P_t^{\text{su}} - P_t^{\text{du}} \quad (9)$$

$$P_t^{\text{md}} = P_t^{\text{sd}} - P_t^{\text{dd}} \quad (10)$$

where  $P_t^{\text{mu}}$  and  $P_t^{\text{md}}$  are the power supply upward and downward adjustment flexibility margins, respectively.

The insufficient upward adjustment flexibility margins are represented by insufficient generating capacity adequacy and upward climbing speed [29]. The power system needs to perform a load shedding action to ensure its normal and stable operation. Insufficient valley-load peak regulation and downward climbing speed are both incidents of insufficient downward adjustment flexibility margins of the power system. The downward adjustment flexibility margins were so tight that the probability of RE consumption was reduced.

## (2) Flexible Adaptability of Grid-Connected RE

Flexible adaptability of grid-connected RE refers to the ability of the power system to accept RE with uncertainty and volatility. In view of the ability of the power system to suppress RE uncertainty fluctuation, two flexible adaptive indices of net load volatility and its maximum volatility were calculated using Equations (11) and (12).

$$V_t^L = (|P_t^{NL} - P_{t-1}^{NL}|) / P_t^{NL} \times 100\% \tag{11}$$

where  $P_t^{NL}$  is the net load and  $V_t^L$  is the net load volatility. The net load volatility refers to the rate of change of the power system's net load. The net load volatility reflects the intensity of fluctuations in the net load per unit time.

$$V_{t,max}^L = \left( \sum_{m_t=1}^{M_t} R_{m_t}^u + \sum_{i=1}^{M_{es}} R_{m_e}^u + R_d^u \right) / P_t^{NL} \times 100\% \tag{12}$$

where  $V_{t,max}^L$  is the maximum allowable volatility of the net load,  $R_{m_e}^u$  is the climbing capability allowed by ES,  $R_d^u$  is the climbing capability allowed by the power system, and  $M_{es}$  is the amount of ES. The greater the maximum allowable volatility of the net load, the stronger the ability of the power system to accept RE. If  $V_{t,max}^L > V_t^L$ , the power system can meet the flexibility requirements. If not, the flexibility of the power system is insufficient.

### 3. Dispatch Model

This paper assumes that all RE is consumed and RE is not used as an optimization variable in dispatch. The prioritized task of FRs is to regulate peak load and try to reduce the peak and valley difference of the net load to improve the flexibility margin. At the same time, the net loads are required to be as flat as possible. A smooth load process is particularly important for TPUs to balance system power. Because the adjustment ability of TPUs is relatively poor, it should bear the base load as much as possible [30].

#### 3.1. Objective Function

This paper considers the joint optimization of ES and interruptible loads under flexibility constraints. ES and interruptible loads are widely used to optimize system flexibility due to their fast response and wide distribution [31]. As illustrated in Figure 2, the overall system consisted of RE composed of wind power and photovoltaic (PV), uninterrupted loads, and FRs (including conventional power sources and flexible dispatch resources). Conventional power sources include TPUs and gas units. Flexible dispatch resources include ES and interruptible loads for participation in system optimal dispatch.

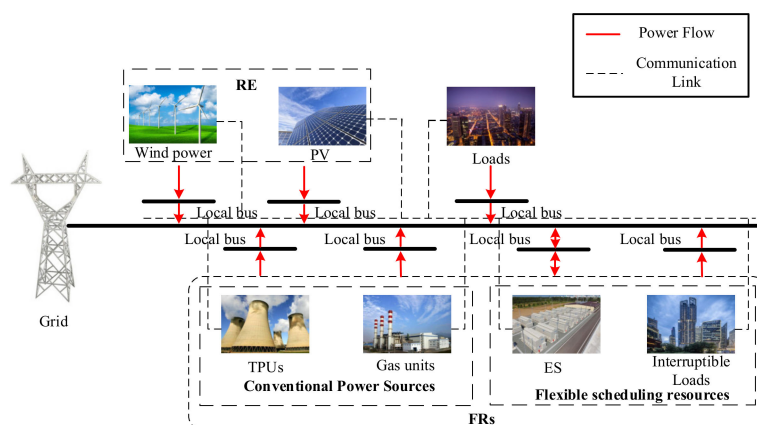


Figure 2. Structural diagram of the overall system.

Compared with other gas units, TPUs emit more  $CO_2$ ,  $SO_2$ , and  $NO_x$  pollutants during operation. In order to minimize the total emission of pollutants during the dispatch period, the system operation

costs and net load volatility should be taken into account. The objective functions are established in Equations (13) and (15).

$$F_1 = \sum_{t=1}^T \sum_{m_t=1}^{M_t} (a_{mt} P_{mt,t}^2 + b_{mt} P_{mt,t} + c_{mt} + d_{mt} e^{\delta_{mt} P_{mt,t}}) \quad (13)$$

$$F_2 = F_E + F_{IL} + F_{ES} + F_F \quad (14)$$

$$F_3 = \sum_{t=1}^T V_t^L \quad (15)$$

where  $F_1$  is the total emissions of pollutants (including  $CO_2$ ,  $SO_2$ , and  $NO_x$ ) in the power system, using tons as the unit,  $F_2$  is the total operation cost, using USD as the unit, and  $F_3$  is the system net load volatility.  $F_2$  includes the cost of purchasing electricity  $F_E$ , the load compensation cost  $F_{IL}$ , the ES operation cost  $F_{ES}$ , and the system prediction error compensation cost  $F_F$ . These costs were calculated using Equations (16) and (19).

$$F_E = \sum_{t=1}^T C_t^E P_t^E \quad (16)$$

$$F_{IL} = \sum_{t=1}^T \sum_{i=1}^{N_{IL}} C_{i,t}^{IL} P_{i,t}^{IL} \quad (17)$$

$$F_{ES} = \sum_{t=1}^T \sum_{i=1}^{N_{ES}} ((C_i^{ES} / M_i^{ES}) P_{i,t}^{ES} \Delta t) \quad (18)$$

$$F_F = \sum_{t=1}^T C_t^F P_t^F \quad (19)$$

where  $C_t^E$  is the unit price of purchased electricity, using USD/MW as the unit,  $P_t^E$  is the purchased electricity,  $C_{i,t}^{IL}$  is compensation time-sharing electricity price of the interruptible loads,  $P_{i,t}^{IL}$  is the consumption of the interruptible loads,  $C_i^{ES}$  is the purchasing cost of the  $i$ -th ES,  $M_i^{ES}$  is the charge and discharge time,  $C_t^F$  is the flexible resource cost, and  $P_t^F$  is the power of FRs.

$E_{CO_2}$ ,  $E_{SO_2}$ , and  $E_{NO_x}$  are the emissions of  $CO_2$ ,  $SO_2$ , and  $NO_x$ . They are obtained by Equations (20) and (22) [32].

$$E_{CO_2} = P_{mt,t} \beta_m Q_{CO_2} \lambda_{CO_2} K_{CO_2} \gamma_{CO_2} \quad (20)$$

$$E_{SO_2} = P_{mt,t} \beta_m \psi_{SO_2} \delta_{SO_2} \gamma_{SO_2} \quad (21)$$

$$E_{NO_x} = 1.63 P_{mt,t} \beta_m (\psi_{NO_x} \delta_{NO_x} + 0.000938) \quad (22)$$

where  $\beta_m$  is the coal consumption rate of power generation,  $Q_{CO_2}$  is the calorific value of coal units,  $\gamma_{CO_2}$  and  $\gamma_{SO_2}$  are the molar mass ratios of  $CO_2$  to C and  $SO_2$  to S, the values of which are 3.67 and 2,  $\lambda_{CO_2}$  is the potential carbon emissions per unit of calorific value,  $K_{CO_2}$  is the oxidation rate of carbon in the fuel,  $\psi_{SO_2}$  and  $\psi_{NO_x}$  are the conversion rates of  $SO_2$  and  $NO_x$  in coal combustion, and  $\delta_{SO_2}$  and  $\delta_{NO_x}$  are the contents of  $SO_2$  and  $NO_x$  in coal combustion.

### 3.2. Constraints

#### (1) Constraints of Power Balance

$$L_t - \sum_{i=1}^{N_{IL}} P_{i,t}^{IL} = P_t^E + \sum_{m_g=1}^{M_g} P_{m_g,t} + \sum_{m_t=1}^{M_t} P_{m_t,t} \pm \sum_{i=1}^{N_{ES}} P_{i,t}^{ES} + P_t^W + P_t^{PV} \quad (23)$$

where  $P_t^w$  is the wind power and  $P_t^{PV}$  is the photovoltaic (PV) power.

(2) Constraints of Upward and Downward Flexibility

$$P_t^{mu} \geq 0 \quad (24)$$

$$P_t^{md} \geq 0 \quad (25)$$

(3) Constraints of Gas Units

Gas units, with a certain adjustable margin, can enhance the anti-disturbance ability of the power system. The daily control power of the gas units is set to a fixed value, as shown in Equation (26).

$$\sum_{t=1}^T P_{m_g,t} \Delta t = E_{m_g} \quad (26)$$

where  $E_{m_g}$  is the daily control power of the gas unit  $m_g$ . The gas units can operate in the load rate range of 0% to 100%. However, when the load rate of the units is less than 75%, their performances are significantly reduced and the cost of power generation is increased, which affects the efficiency of power generation. Therefore, this paper sets the load rate of 75% as the lower limit of the output power of gas units, as shown in Equations (27) and (28).

$$P_{m_g}^- \leq P_{m_g,t} \leq P_{m_g}^+ \quad (27)$$

$$P_{m_g}^- = \max(P_{m_g}^-, 0.75P_{m_g}^+) \quad (28)$$

Meanwhile, frequent starts and stops significantly affect the lives of the gas units and increase operation costs. Therefore, we set the minimum start-up duration to avoid frequent starts and stops of gas units, as shown in Equation (29).

$$t_{m_g} \geq t_{m_g}^- \quad (29)$$

$$P_{m_g,t+1} - P_{m_g,t} \leq R_{m_g}^u, P_{m_g,t+1} - P_{m_g,t} \geq 0 \quad (30)$$

$$P_{m_g,t} - P_{m_g,t+1} \leq R_{m_g}^d, P_{m_g,t} - P_{m_g,t+1} \geq 0 \quad (31)$$

where  $t_{m_g}$  is the continuous operation time of the gas unit  $m_g$ , using h as the unit,  $t_{m_g}^-$  is the minimum operation time.

(4) Constraints of TPUs

$$u_{m_t,1} = u_{m_t,2} = \dots = u_{m_t,T} \quad (32)$$

Other constraints of the TPU, such as the upper and lower limits of the output force and the ability to climb the slope, are the same as those of the gas unit.

(5) Constraints of Interruptible Loads

$$P_{i,\min,t}^{IL} \leq P_{i,t}^{IL} \leq P_{i,\max,t}^{IL} \quad (33)$$

$$T_{i,\min}^{IL} \leq T_i^{IL} \leq T_{i,\max}^{IL} \quad (34)$$

where  $P_{i,\min,t}^{IL}$  and  $P_{i,\max,t}^{IL}$  are the minimum and maximum values of the interruptible loads and  $T_{i,\min}^{IL}$  and  $T_{i,\max}^{IL}$  are the minimum and maximum times.

(6) Constraints of ES

The remaining capacity of the ES, the state of charge (SOC), is not only related to the current dispatch, but also affects its next dispatch. SOC reflects the ratio of the ES remaining capacity to the total capacity in the current period. Therefore, the state of charge of ES is a key variable in the process of charging and discharging. The SOC constraint equation is expressed in Equation (35).

$$SOC_{\min,i} \leq SOC_i \leq SOC_{\max,i} \tag{35}$$

where  $SOC_{\min,i}$  and  $SOC_{\max,i}$  are lower and upper limits of the SOC for  $i$ -th ES.

The three weight coefficients are related to pollution emissions, total operation cost, and net load volatility, respectively. If the weight  $F_1$  of pollution emissions is higher, it will lead to insufficient utilization of FRs in optimal dispatch. If the weights  $F_2$  and  $F_3$  of total operation cost and net load volatility are higher, the economic cost of the system will be increased. The three weights can be relatively flexibly chosen, according to the demands and conditions of the power system. In this paper, the weights of  $F_1$ ,  $F_2$ , and  $F_3$  were chosen as 0.5, 0.25, and 0.25. However, our approach was not limited to this set of parameters.

The overall flow chart of the proposed framework of optimal dispatch is shown in Figure 3. The comprehensive flexibility evaluation indices, including the power supply flexibility margin and the flexible adaptability of grid-connected RE, were developed. Insufficient upward adjustment flexibility margins will lead to load shedding. Insufficient downward adjustment flexibility margins may reduce consumption of RE. Insufficient flexible adaptability of grid-connected RE will change net load volatility. The optimal targets consider pollutant emissions, operation cost, and net load volatility. A dispatch model with ES and interruptible loads was constructed based on the proposed power system flexibility evaluation indices and constraints.

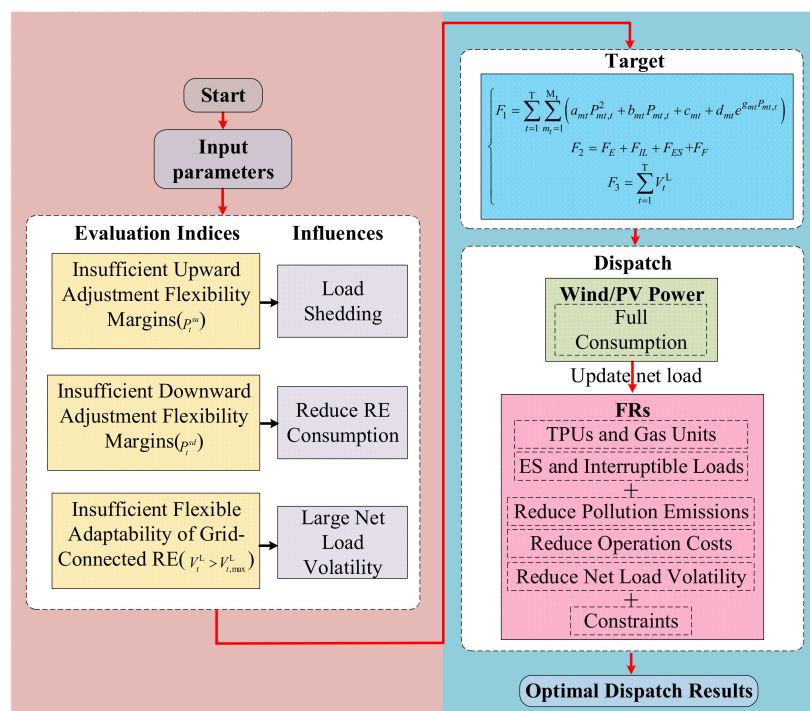


Figure 3. The overall flow chart of the proposed framework of optimal dispatch.

#### 4. Analysis of Examples

##### 4.1. The Setup of Simulation

The volatility and variability of RE have made the demand for flexibility in the high-penetration integrated power system significantly increase. On the premise of ensuring the safe operation of the

power system, we gradually increased the penetration rate of RE. The resulting net load curve is shown in Figure 4.

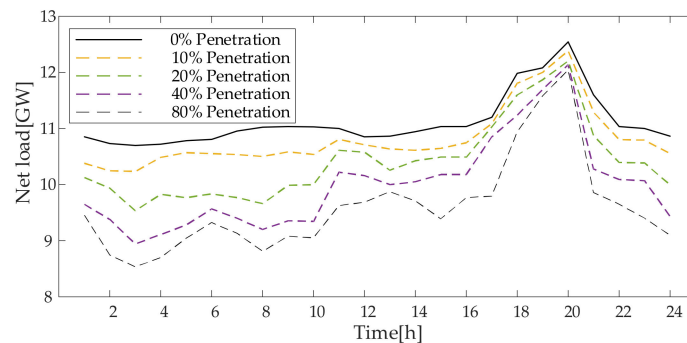


**Figure 4.** Net load curves with different renewable energy (RE) penetrations.

As shown in Figure 4, with the gradual increase in the penetration rate of RE, there were three changes in the net load curves:

- (1) During 02:00–04:00, with increasing penetration rate, the net load valley reduced, which lead to insufficient flexibility in the downward adjustment of the power system.
- (2) During 16:00–20:00, with increasing penetration rate, the net load fluctuation rate increased, causing the system net load fluctuation rate insufficient flexibility.
- (3) During 19:00–21:00, with increasing penetration rate, the peak of the net load decreased, which had a certain effect on improving the upward flexibility of the power system.

Figure 5 shows the total load, wind power, and PV curves during 1 week. The output of wind power fluctuated and the power of PV was 0 in the morning and evening. Due to the habits of consumers, the valley period of the total load was in the evening and the peak period of the total load was in the morning. Compared with the working day, the total load on Saturday and Sunday was lower. There were four TPUs and one gas unit in the test system. This paper focuses on the regulation of flexibility, and the predicted values of wind power and PV were used as actual values in model dispatch. The parameters are shown in Table 2. The pollution emission coefficients  $a_{mt}$ ,  $b_{mt}$ ,  $c_{mt}$ ,  $d_{mt}$ , and  $g_{mt}$  of the TPUs were obtained by fitting the actual emission data of the units. The TPUs, gas units, and interruptible loads parameters  $P_{m_t}^+$ ,  $P_{m_t}^-$ ,  $P_{m_g}^+$ ,  $P_{m_g}^-$ ,  $R_{m_t}^u$ ,  $R_{m_g}^d$ ,  $P_{i,\min,t}^{IL}$ ,  $P_{i,\max,t}^{IL}$ ,  $t_{m_g}^-$ ,  $T_{i,\min}^{IL}$ , and  $T_{i,\max}^{IL}$  were obtained from a provincial power grid in China. The rest of the parameters refer to [33–35] and were set according to the actual operation of the power grid. The initial state of charge (SOC) of ES is 0.5 [35].

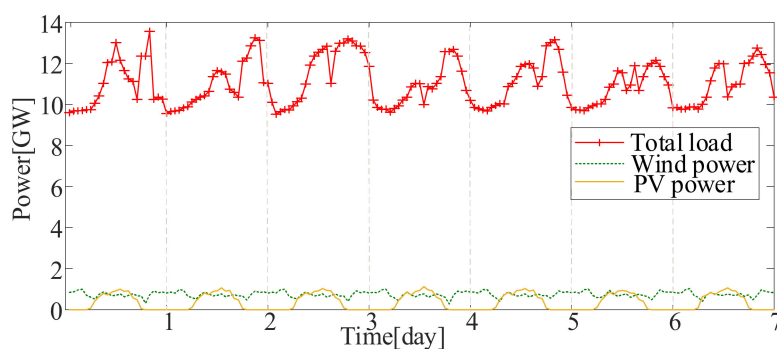


**Figure 5.** The prediction curves of total load, wind power and photovoltaic (PV) power.

**Table 2.** The parameters of dispatch models.

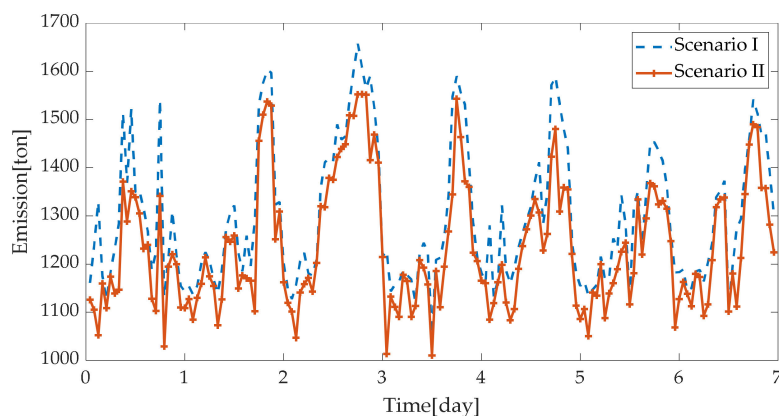
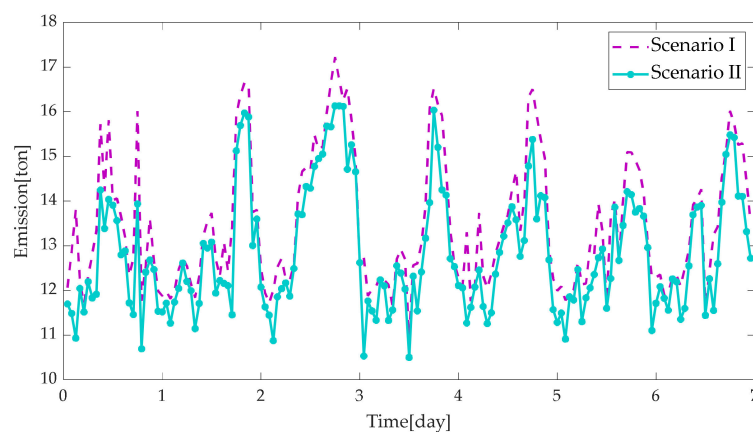
Parameter	Value	Parameter	Value	Parameter	Value	Parameter	Value
$a_{mt}$ (kg/MW <sup>2</sup> )	0.0135	$R_{m_t}^u$ (MW/h)	1000	$\lambda_{CO_2}$ (t/TJ)	27.74	$C_{i,t}^{IL}$ (USD/MW)	5
$b_{mt}$ (kg/MW)	-2.22	$R_{m_g}^d$ (MW/h)	100	$K_{CO_2}$ (%)	0.9	$C_i^{ES}$ (USD/MW)	30,000
$c_{mt}$ (kg)	300	$P_{i,min,t}^{IL}$ (MW)	0	$\psi_{SO_2}$ (%)	90	$C_t^F$ (USD/MW)	6
$d_{mt}$ (kg)	0.5035	$P_{i,max,t}^{IL}$ (MW)	300	$\delta_{SO_2}$ (%)	1	$M_i^{ES}$ (day)	2000
$g_{mt}$ (MW <sup>-1</sup> )	0.0208	$t_{m_g}^-$ (h)	2	$\psi_{NO_x}$ (%)	25	$M_g$	2
$P_{m_t}^+$ (MW)	3000	$T_{i,min}^{IL}$ (h)	0	$\delta_{NO_x}$ (%)	1.5	$M_t$	4
$P_{m_t}^-$ (MW)	1500	$T_{i,max}^{IL}$ (h)	8	$SOC_{min,i}$	0.2	$N_{IL}$	2
$P_{m_g}^+$ (MW)	500	$\beta_m$ (g/KWh)	300	$SOC_{max,i}$	0.9	$N_{ES}$	2
$P_{m_g}^-$ (MW)	300	$Q_{CO_2}$ (MJ/kg)	21.2	$C_t^E$ (USD/MW)	5	-	-

#### 4.2. Comparison of Different Dispatch Models

This paper compares two scenarios to verify the effectiveness of the proposed dispatch model with flexibility indices in the high-penetration RE integrated power system.

In scenario I, no FRs were used. In scenario II, ES and interruptible loads were dispatched.

Figures 6–8 show the comparison of the emissions of CO<sub>2</sub>, SO<sub>2</sub>, and NO<sub>x</sub> under the two scenarios. Due to comprehensive flexibility evaluation indices and constraints, the output of TPUs and FRs were adjusted. The output of TPUs was reduced, thanks to the utilization of FRs in the model. Compared with scenario I, the emissions of CO<sub>2</sub>, SO<sub>2</sub>, and NO<sub>x</sub> in scenario II decreased by an average of 62.15 tons, 0.65 tons, and 0.27 tons, respectively. The total pollutant emission decreased by 63.07 tons, and the emission reduction rate was 4.8%.

**Figure 6.** Comparison of CO<sub>2</sub> emission.**Figure 7.** Comparison of SO<sub>2</sub> emission.

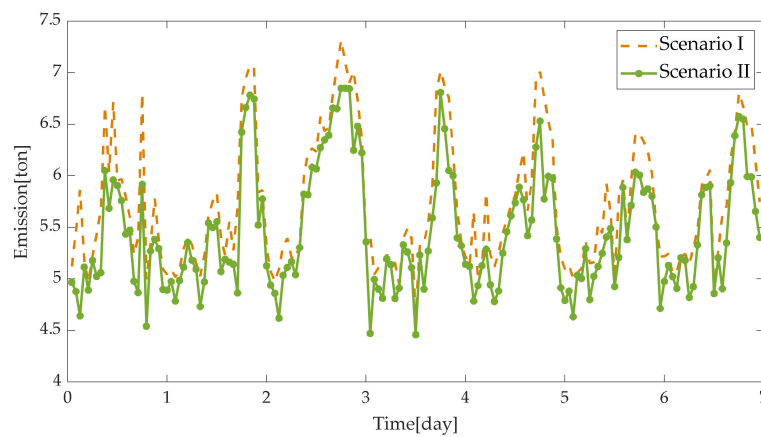


**Figure 8.** Comparison of  $NO_x$  emission.

#### 4.3. Analysis of Dispatch Results of One Day

In scenario I, no FR participated in the optimal dispatch model. The flexibility of the power system was adjusted by traditional resources. In scenario II, ES and interruptible loads were dispatched to enhance the flexibility. The coordination of FRs and traditional resources was used to increase the capacity of RE consumption. The difference between the models in the two scenarios was whether to utilize FRs. Based on the proposed flexibility evaluation indices, the FRs were used to reduce the peak-valley difference of the net load and the net load fluctuation rate. Therefore, compared with scenario I, the average output of the TPUs in scenario II could be reduced and the system's flexibility margin was increased.

Figure 9 shows the upward and downward flexibility margin of the power system. In scenario I, the flexibility redundancy during the peak-load period was large. There was a lack of flexibility margin in the valley-load period. The flexibility deviations during 04:00–05:00 reached 92.56 MW and 113.57 MW, respectively. Figure 8 indicates that the power system had insufficient downward adjustment during 04:00–05:00, which caused the power system to not respond to the changes of load and RE quickly. There was a high probability of causing wind curtailment or emergency shutdown of TPUs.

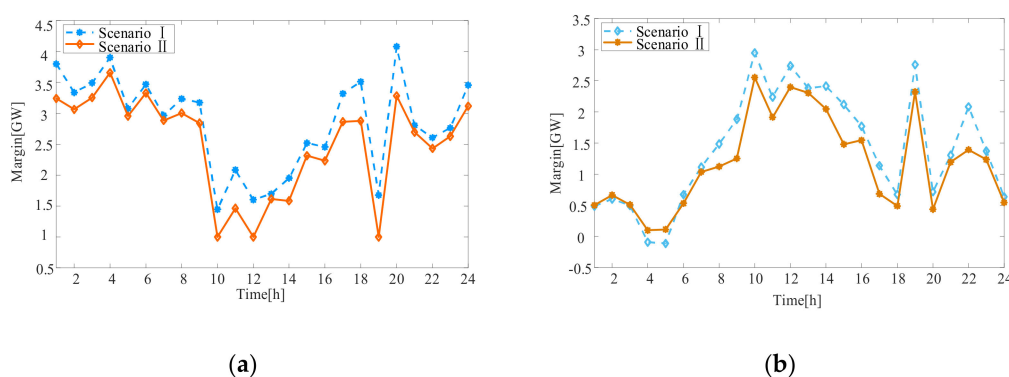


**Figure 9.** Comparison of flexibility margins between the two scenarios. (a) Upward flexibility margin. (b) Downward flexibility margin.

In scenario II, the FRs were adjusted according to the power supply flexibility margin indices. The system's downward flexibility requirements in the valley-load period and its adjacent period were considered. By exploiting the flexibility of upward adjustment of FRs during the peak-load time, the system could meet the flexibility requirements of each period.

With the optimal dispatch of FRs, the flexibility of the power system with a high-penetration RE was significantly improved. Figure 10 shows the comparison curves of the net load change under two scenarios.

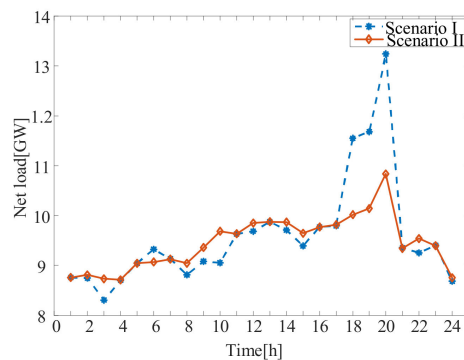


**Figure 10.** Net load change curves of two scenarios.

As can be seen from Figure 10, when the FRs participated in the optimal dispatch, the trend of the net load changed relatively slowly and the difference between the peak and valley loads reduced. Especially during 17:00–21:00, the net load fluctuation in scenario II was significantly less than that in scenario I. Net load fluctuation slowed significantly. The TPUs had relatively poor adjustment capability and could only bear the base load. The FRs could minimize the difference between the peak and valley of the net load. Thus, enhancing the flexibility of the system can reduce the output of TPUs and pollutant emissions.

Figure 11 shows the net allowable volatility curve and the net load volatility curve for 24 h in the two scenarios. At 19:00 and 20:00, the net load volatility exceeded the maximum net load volatility allowed in scenario I. At this time, the power system was insufficiently flexible and the peak-load regulation ability was weak. In order to ensure the stable operation of the power system, we performed operations such as abandoning wind, discarding light, and removing the load. In scenario II with FRs participating in optimal dispatch, the maximum allowable net load volatility was significantly improved and the net load volatility indices at each moment were met. The net load volatility at 20:00 decreased from 28.55% in scenario I to 16.01% and, at other time points, the net load volatility of scenario II was significantly lower than scenario I.

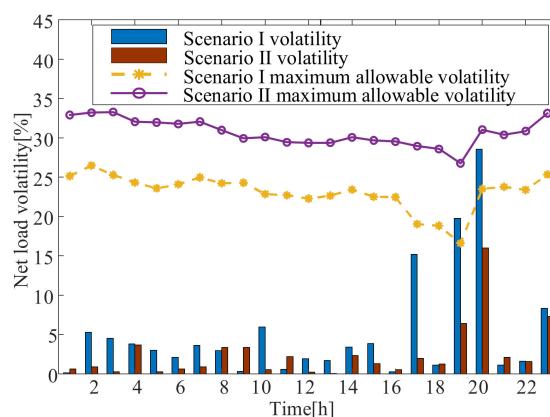


**Figure 11.** Net load volatility curves of two scenarios.

Under the optimal dispatch of FRs, the output of TPUs reduced. While saving costs, the coal consumption of TPUs also decreased, so that the total amount of pollutants reduced. We analyzed the impact of interruptible loads and ES on pollutant emissions, total operation costs, and net load volatility.

The results of the TPUs optimization of two scenarios are shown in Figure 12. The interruptible loads and ES optimal results are shown in Figures 13 and 14.

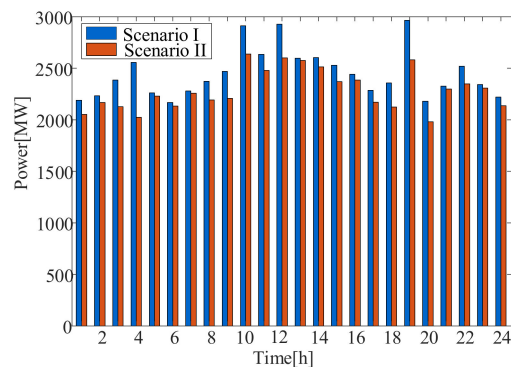


**Figure 12.** Results of coordinated optimal dispatch of thermal power units (TPUs).

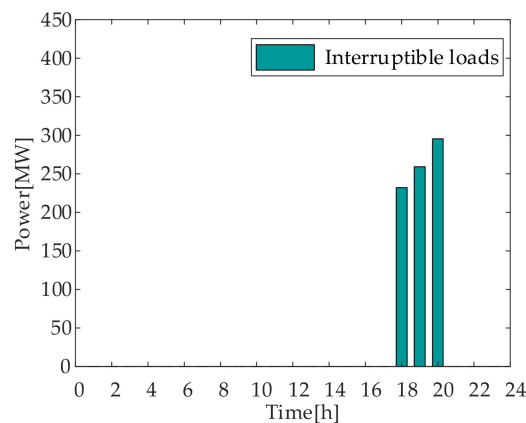


**Figure 13.** Result of interruptible loads optimal dispatch.

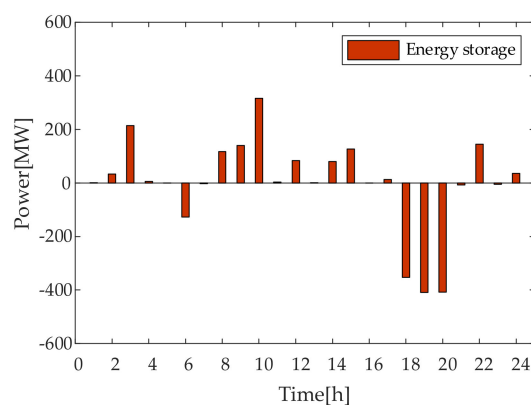


**Figure 14.** Result of energy storage optimal dispatch.

Figures 12–14 show the power curves of TPUs, ES, and interruptible loads, respectively. In scenario II, FRs and traditional resources participated in optimal dispatch. During periods of peak load (10:00–19:00), FRs and traditional resources were coordinated to reduce the volatility caused by RE and reduce the output of TPUs. During periods of valley load (00:00–06:00), ES used its rapid response to fill the net load valley. In scenario I, the output of the TPUs was higher than that in scenario II, since only traditional resources were adjusted in optimal dispatch. Thanks to FRs, the output power of the TPU was smoothed to enhance stability. It can be seen from Figure 12 that the maximum

output of TPUs was 2.64 GW, the peak-to-valley difference reduced from 0.90 GW to 0.66 GW, and the mean square error reduced from 2.56 GW to 2.02 GW, which verifies the proposed model.

The total operating costs of scenario I and scenario II were 223,720 USD and 195,240 USD, respectively. The average daily production of TPUs was 2.51 GW and 2.29 GW. The total pollution emission reduced from 6008.77 tons to 5492.49 tons and the emission reduction rate was 8.5%. These results mainly benefit from the flexibility indices proposed in this paper. Through the optimization of limited flexibility resources, system redundancy greatly decreased. The TPUs output and pollutant emissions were also reduced.

Figures 15 and 16 show the comparisons of  $CO_2$ ,  $SO_2$ , and  $NO_x$  emissions, respectively.

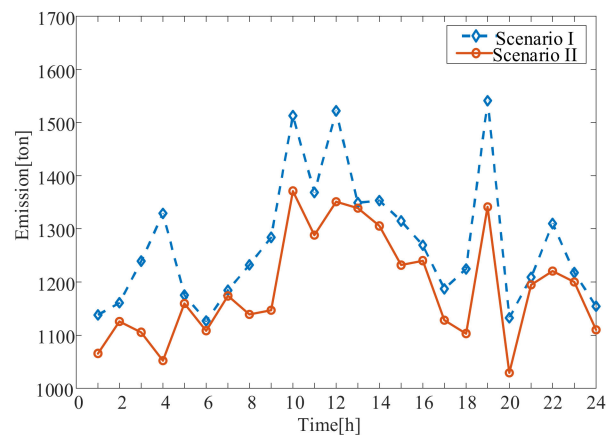


Figure 15. The emission of  $CO_2$ .

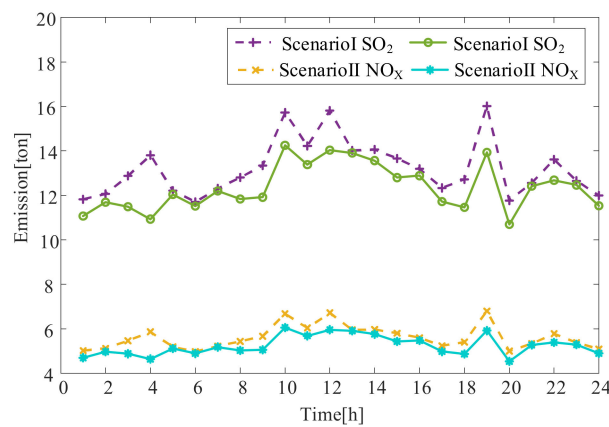


Figure 16. The emissions of  $SO_2$  and  $NO_x$ .

Figures 15 and 16 show that the pollutant emissions in scenario II were lower than scenario I in 24 h. It shows that under the optimal dispatch of FRs, it can effectively reduce the emissions of  $CO_2$ ,  $SO_2$ , and  $NO_x$ . It proves that flexible resource optimal dispatch can meet the requirements of reducing fluctuation of net load and pollutant emission in the power system with high-penetration RE.

## 5. Conclusions

This paper proposes comprehensive flexibility evaluation indices to enhance the flexibility of a power system. The developed dispatch model considers FRs and quantifies the power system flexibility in terms of time scale and directionality. Our method improves the flexibility margin of the power system and reduces pollution emissions. Compared with the traditional optimal dispatch method, the average daily emissions of  $CO_2$ ,  $SO_2$ , and  $NO_x$ , with the proposed optimal method,

are reduced by 83.60 tons, 0.87 tons, and 0.37 tons, the maximum allowable fluctuation rate of the net load increases by 7.63%, and the average volatility of the net load decreases by 2.67%.

We will try our best to apply the proposed method in a real case study to further verify its effectiveness in future work.

**Author Contributions:** Conceptualization, J.F.; Formal analysis, H.W. and H.J.; Methodology, W.G. and B.H.; Project administration, G.W.; Resources, M.O.O.; Supervision, J.Y.; Validation, J.C.; Writing—original draft, J.W. All authors have read and agreed to the published version of the manuscript.

**Funding:** This work was funded by the China Postdoctoral Science Foundation under Grant 2019M651144, in part by the Liaoning Provincial Department of Education Research Funding under Grant LQGD2019005, in part by Liaoning Provincial Doctoral Research Start-up Funding Project under Grant 2020-BS-141.

**Conflicts of Interest:** The authors declare no conflict of interest.

## Nomenclature

The following nomenclatures are used in this manuscript:

RE	Renewable energy
FRs	Flexible Resources
ES	Energy storage
TPU	Thermal power unit
SOC	State of charge
PV	Photovoltaic
$P_t^{su} / P_t^{sd}$	Upward/downward adjustment flexibilities of system
$M_t$	Total number of TPUs
$P_{m_t,t}^u / P_{m_t,t}^d$	Upward/Downward adjustment flexibilities of TPU $m_t$
$P_{m_t,t}$	The output of TPU $m_t$
$P_{m_t}^+ / P_{m_t}^-$	Upper/Lower limits of the output of TPU $m_t$
$R_{m_t}^u / R_{m_t}^d$	Climbing/Descending capabilities of TPU $m_t$
$M_g$	Total number of gas units
$P_{m_g,t}^u / P_{m_g,t}^d$	Upward/downward adjustment flexibilities of the gas unit $m_g$
$P_{m_g,t}$	The output of the gas unit $m_g$
$P_{m_g}^+ / P_{m_g}^-$	Upper/Lower limits of the output of the gas unit $m_g$
$R_{m_g}^u / R_{m_g}^d$	Climbing/Descending capabilities of the gas unit $m_g$
$P_t^{du} / P_t^{dd}$	Requirements of power system upward/downward adjustment flexibilities
$w_u / w_d$	Requirements of wind power prediction error for upward/ downward adjustment flexibilities
$P_t^w$	Wind power prediction
$P_{\max}^w$	Maximum wind power prediction
$n_u / n_d$	Requirements of the system load forecasting error for the upward/ downward adjustment flexibilities
$P_t^{mu} / P_t^{md}$	Power supply upward/downward adjustment flexibility margins
$V_t^L$	Net load volatility
$P_t^{NL}$	Net load
$V_{t,\max}^L$	Maximum allowable volatility of the net load
$R_{m_e}^u$	Ability to climb the slope allowed by ES
$R_d^u$	Climbing ability allowed by the power system
$F_1$	Total emissions of pollutants
$F_2$	Total operation cost
$F_3$	System net load volatility
$F_E$	Purchasing of electricity cost
$F_{IL}$	Load compensation cost
$F_{ES}$	ES operation cost
$F_F$	System prediction error compensation cost
$C_t^E$	The unit price of purchasing electricity

$P_t^E$	Purchasing electricity
$C_{i,t}^{IL}$	Interruptible loads compensation time-sharing electricity price
$P_{i,t}^{IL}$	Consumption of the interruptible loads
$C_i^{ES}$	The $i$ -th ES purchasing cost
$M_i^{ES}$	Charge and discharge times
$C_t^F$	Flexible resource cost
$P_t^F$	FRs required to stabilize the prediction error
$E_{CO_2}/E_{SO_2}/E_{NO_x}$	Emissions of $CO_2/SO_2/NO_x$
$\beta_m$	The coal consumption rate of power generation
$Q_{CO_2}$	The calorific value of coal units
$\lambda_{CO_2}$	Potential carbon emissions per unit of calorific value
$K_{CO_2}$	The oxidation rate of carbon in the fuel
$\psi_{SO_2}/\psi_{NO_x}$	Conversion rates of $SO_2/NO_x$
$\delta_{SO_2}/\delta_{NO_x}$	Contents of $SO_2/NO_x$ in coal combustion
$P_t^W$	Power of the wind turbine
$P_t^{PV}$	Power of the PV
$E_{m_g}$	Daily control power of the gas unit $m_g$
$t_{m_g}$	Continuous operation time of the gas unit $m_g$
$t_{m_g}^-$	Minimum operation time
$u_{m_i,t}$	The 0, 1 variable of the unit startup state
$P_{i,\min,t}^{IL}/P_{i,\max,t}^{IL}$	Minimum/Maximum values of the interruptible loads
$T_{i,\min}^{IL}/T_{i,\max}^{IL}$	Minimum/Maximum times
$SOC_{\min,i}/SOC_{\max,i}$	Lower/Upper limits of the SOC

## References

- Shi, Y.; Xu, B.; Wang, D.; Zhang, B. Using Battery Storage for Peak Shaving and Frequency Regulation: Joint Optimization for Superlinear Gains. *IEEE Trans. Power Syst.* **2018**, *33*, 2882–2954. [[CrossRef](#)]
- Wang, H.; Yang, J.; Chen, Z.; Li, G.; Liang, J.; Ma, Y.; Dong, H.; Ji, H.; Feng, J. Optimal dispatch based on prediction of distributed electric heating storages in combined electricity and heat networks. *Appl. Energy* **2020**, *267*, 114879. [[CrossRef](#)]
- Wang, Q.; Hodge, B.-M.S. Enhancing Power System Operational Flexibility with Flexible Ramping Products: A Review. *IEEE Trans. Ind. Inform.* **2016**, *13*. [[CrossRef](#)]
- Mohandes, B.; El Moursi, M.S.; Hatziargyriou, N.; El Khatib, S. A Review of Power System Flexibility with High Penetration of Renewables. *IEEE Trans. Power Syst.* **2019**, *34*, 3140–3155. [[CrossRef](#)]
- Zhou, M.; Zhai, J.; Li, G.; Ren, J. Distributed Dispatch Approach for Bulk AC/DC Hybrid Systems with High Wind Power Penetration. In Proceedings of the IEEE Power and Energy Society General Meeting (PESGM), Portland, OR, USA, 5–10 August 2018.
- Taha, M.S.; Abdeltawab, H.H.; Mohamed, Y.A.-R.I. An Online Energy Management System for a Grid-Connected Hybrid Energy Source. *IEEE J. Emerg. Sel. Top. Power Electron.* **2018**, *6*, 2015–2030. [[CrossRef](#)]
- Khorramdel, B.; Chung, C.Y.; Safari, N.; Price, G.D. A Fuzzy Adaptive Probabilistic Wind Power Prediction Framework Using Diffusion Kernel Density Estimators. *IEEE Trans. Power Syst.* **2018**, *33*, 7109–7121. [[CrossRef](#)]
- Wu, T.-F.; Misra, M.; Lin, L.-C.; Hsu, C.-W. An Improved Resonant Frequency Based Systematic LCL Filter Design Method for Grid-Connected Inverter. *IEEE Trans. Ind. Electron.* **2017**, *64*, 6412–6421. [[CrossRef](#)]
- Chen, H.; Zhang, R.; Bai, L.; Li, G.; Li, F. Economic dispatch of wind integrated power systems with energy storage considering composite operating costs. *IET Gener. Transm. Distrib.* **2016**, *10*, 1294–1303. [[CrossRef](#)]
- Karthikeyan, N.; Pillai, J.R.; Bak-Jensen, B.; Simpson-Porco, J.W.; Nainar, K. Predictive Control of Flexible Resources for Demand Response in Active Distribution Networks. *IEEE Trans. Power Syst.* **2019**, *34*, 2957–2969. [[CrossRef](#)]
- Asl, D.K.; Hamed, A.; Seifi, A.R. Planning, operation and flexibility contribution of multi-carrier energy storage systems in integrated energy systems. *IET Renew. Power Gener.* **2020**, *14*, 408–416. [[CrossRef](#)]

12. Gottwalt, S.; Gartner, J.; Schmeck, H.; Weinhardt, C. Modeling and Valuation of Residential Demand Flexibility for Renewable Energy Integration. *IEEE Trans. Smart Grid* **2016**, *8*, 2565–2574. [[CrossRef](#)]
13. Mhanna, S.; Chapman, A.C.; Verbič, G. A Faithful and Tractable Distributed Mechanism for Residential Electricity Pricing. *IEEE Trans. Power Syst.* **2017**, *33*, 4238–4252. [[CrossRef](#)]
14. Lei, S.; Hou, Y.; Wang, X.; Liu, K. Unit Commitment Incorporating Spatial Distribution Control of Air Pollutant Dispersion. *IEEE Trans. Ind. Inform.* **2017**, *13*, 995–1005. [[CrossRef](#)]
15. Bruce, A.R.W.; Gibbins, J.; Harrison, G.P.; Chalmers, H.; Gibbins, J. Operational Flexibility of Future Generation Portfolios Using High Spatial- and Temporal-Resolution Wind Data. *IEEE Trans. Sustain. Energy* **2015**, *7*, 697–707. [[CrossRef](#)]
16. Wang, S.; Bi, S.; Zhang, Y.J. Demand Response Management for Profit Maximizing Energy Loads in Real-Time Electricity Market. *IEEE Trans. Power Syst.* **2018**, *33*, 6387–6396. [[CrossRef](#)]
17. Good, N.; Mancarella, P. Flexibility in Multi-Energy Communities With Electrical and Thermal Storage: A Stochastic, Robust Approach for Multi-Service Demand Response. *IEEE Trans. Smart Grid* **2017**, *10*, 503–513. [[CrossRef](#)]
18. Zhang, X.; Hug, G.; Kolter, J.Z.; Harjunkoski, I.; Kolter, Z. Demand Response of Ancillary Service From Industrial Loads Coordinated With Energy Storage. *IEEE Trans. Power Syst.* **2017**, *33*, 951–961. [[CrossRef](#)]
19. Chen, X.; Lv, J.; McElroy, M.; Han, X.; Nielsen, C.P.; Wen, J. Power System Capacity Expansion Under Higher Penetration of Renewables Considering Flexibility Constraints and Low Carbon Policies. *IEEE Trans. Power Syst.* **2018**, *33*, 6240–6253. [[CrossRef](#)]
20. Bistline, J.E. Turn Down for What? The Economic Value of Operational Flexibility in Electricity Markets. *IEEE Trans. Power Syst.* **2018**, *34*, 527–534. [[CrossRef](#)]
21. Ahmad, N.; Jamshid, A.; Miadreza, S.K.; Catalao, J.P.S. Assessing Increased Flexibility of Energy Storage and Demand Response to Accommodate a High Penetration of Renewable Energy Sources. *IEEE Trans. Sustain. Energy* **2019**, *10*, 659–669.
22. Tejada-Arango, D.A.; Morales-España, G.; Wogrin, S.; Centeno, E. Power-Based Generation Expansion Planning for Flexibility Requirements. *IEEE Trans. Power Syst.* **2020**, *35*, 2012–2023. [[CrossRef](#)]
23. Di Somma, M.; Graditi, G.; Siano, P. Optimal Bidding Strategy for a DER Aggregator in the Day-Ahead Market in the Presence of Demand Flexibility. *IEEE Trans. Ind. Electron.* **2018**, *66*, 1509–1519. [[CrossRef](#)]
24. Zhao, J.; Zheng, T.; Litvinov, E. A Unified Framework for Defining and Measuring Flexibility in Power System. *IEEE Trans. Power Syst.* **2015**, *31*, 339–347. [[CrossRef](#)]
25. He, L.; Li, Y.; Shuai, Z.; Guerrero, J.M.; Cao, Y.; Wen, M.; Wang, W.; Shi, J. A Flexible Power Control Strategy for Hybrid AC/DC Zones of Shipboard Power System with Distributed Energy Storages. *IEEE Trans. Ind. Inform.* **2018**, *14*, 5496–5508. [[CrossRef](#)]
26. Jahid, A.; Monju, K.H.; Hossain, E.; Hossain, F. Renewable Energy Assisted Cost Aware Sustainable Off-Grid Base Stations with Energy Cooperation. *IEEE Access* **2018**, *6*, 60900–60920. [[CrossRef](#)]
27. Zhang, Z.; Chen, Q.; Xie, R.; Sun, K. The Fault Analysis of PV Cable Fault in DC Microgrids. *IEEE Trans. Energy Convers.* **2018**, *34*, 486–496. [[CrossRef](#)]
28. Wang, H.; Yang, J.; Chen, Z.; Ge, W.; Ma, Y.; Xing, Z.; Yang, L. Model Predictive Control of PMSG-Based Wind Turbines for Frequency Regulation in an Isolated Grid. *IEEE Trans. Ind. Appl.* **2018**, *54*, 3077–3089. [[CrossRef](#)]
29. Lu, Z.; Li, H.; Qiao, Y. Probabilistic Flexibility Evaluation for Power System Planning Considering Its Association with Renewable Power Curtailment. *IEEE Trans. Power Syst.* **2018**, *33*, 3285–3295. [[CrossRef](#)]
30. Chen, Y.; Yu, T.; Yang, B.; Zhang, X.; Qu, K. Many-Objective Optimal Power Dispatch Strategy Incorporating Temporal and Spatial Distribution Control of Multiple Air Pollutants. *IEEE Trans. Ind. Inform.* **2019**, *15*, 5309–5319. [[CrossRef](#)]
31. Nosair, H.; Bouffard, F. Energy-Centric Flexibility Management in Power Systems. *IEEE Trans. Power Syst.* **2016**, *31*, 5071–5081. [[CrossRef](#)]
32. Hao, P.; Wu, G.; Boriboonsomsin, K.; Barth, M.J. Eco-Approach and Departure (EAD) Application for Actuated Signals in Real-World Traffic. *IEEE Trans. Intell. Transp. Syst.* **2018**, *20*, 30–40. [[CrossRef](#)]

33. Konstantelos, I.; Giannelos, S.; Strbac, G. Strategic Valuation of Smart Grid Technology Options in Distribution Networks. *IEEE Trans. Power Syst.* **2018**, *32*, 1293–1303.
34. Yuan, C.; Gu, C.; Li, F.; Kuri, B.; Dunn, R.W. New Problem Formulation of Emission Constrained Generation Mix. *IEEE Trans. Power Syst.* **2013**, *28*, 4064–4071. [[CrossRef](#)]
35. Li, W.; Li, T.; Wang, H.; Dong, J.; Li, Y.; Cui, D.; Ge, W.; Yang, J.; Okoye, M.O. Optimal Dispatch Model Considering Environmental Cost Based on Combined Heat and Power with Thermal Energy Storage and Demand Response. *Energies* **2019**, *12*, 817. [[CrossRef](#)]



© 2020 by the authors. Licensee MDPI, Basel, Switzerland. This article is an open access article distributed under the terms and conditions of the Creative Commons Attribution (CC BY) license (<http://creativecommons.org/licenses/by/4.0/>).